



# <sup>18</sup>F-FDG PET metabolic-to-morphological volume ratio predicts PD-L1 tumour expression and response to PD-1 blockade in non-small-cell lung cancer

Mario Jreige<sup>1</sup> · Igor Letovanec<sup>2</sup> · Kariman Chaba<sup>3</sup> · Stephanie Renaud<sup>3</sup> · Sylvie Rusakiewicz<sup>3</sup> · Valerie Cristina<sup>4</sup> · Solange Peters<sup>5</sup> · Thorsten Krueger<sup>6</sup> · Laurence de Leval<sup>2</sup> · Lana E. Kandalaft<sup>3</sup> · Marie Nicod-Lalonde<sup>1</sup> · Pedro Romero<sup>4</sup> · John O. Prior<sup>1</sup> · George Coukos<sup>3,4</sup> · Niklaus Schaefer<sup>1</sup>

Received: 17 December 2018 / Accepted: 29 April 2019 / Published online: 18 June 2019  
© Springer-Verlag GmbH Germany, part of Springer Nature 2019

## Abstract

**Purpose** Anti-PD-1/PD-L1 blockade can restore tumour-specific T-cell immunity and is an emerging therapy in non-small-cell lung cancer (NSCLC). We investigated the correlation between <sup>18</sup>F-FDG PET/CT-based markers and tumour tissue expression of PD-L1, necrosis and clinical outcome in patients receiving checkpoint inhibitor treatment.

**Methods** PD-L1 expression in biopsy or resection specimens from 49 patients with confirmed NSCLC was investigated by immunohistochemistry. Maximum standardized uptake value (SUVmax), mean SUV (SUVmean), metabolic tumour volume (MTV) and total lesion glycolysis (TLG) were obtained from <sup>18</sup>F-FDG PET/CT images. The ratio of metabolic to morphological lesion volumes (MMVR) and its association with PD-L1 expression in each lesion were calculated. The associations between histologically reported necrosis and <sup>18</sup>F-FDG PET imaging patterns and radiological outcome (evaluated by iRECIST) following anti-PD-1/PD-L1 therapy were also analysed. In 14 patients, the association between necrosis and MMVR and tumour immune contexture were analysed by multiple immunofluorescent (IF) staining for CD8, PD-1, granzyme B (GrzB) and NFATC2.

**Results** In total, 25 adenocarcinomas and 24 squamous cell carcinomas were analysed. All tumours showed metabolic <sup>18</sup>F-FDG PET uptake. MMVR was correlated inversely with PD-L1 expression in tumour cells. Furthermore, PD-L1 expression and low MMVR were significantly correlated with clinical benefit. Necrosis was correlated negatively with MMVR. Multiplex IF staining showed a greater frequency of activated CD8<sup>+</sup> cells in necrotic tumours than in nonnecrotic tumours in both stromal and epithelial tumour compartments.

**Conclusion** This study introduces MMVR as a new imaging biomarker and its ability to noninvasively capture increased PD-L1 tumour expression and predict clinical benefit from checkpoint blockade in NSCLC should be further evaluated.

**Keywords** FDG · PET/CT · PD-L1 · Imaging · NSCLC

---

This article is part of the Topical Collection on Oncology – Chest

**Electronic supplementary material** The online version of this article (<https://doi.org/10.1007/s00259-019-04348-x>) contains supplementary material, which is available to authorized users.

---

✉ Niklaus Schaefer  
niklaus.schaefer@chuv.ch

<sup>1</sup> Department of Nuclear Medicine and Molecular Imaging, Lausanne University Hospital, Rue du Bugnon 46, CH-1011 Lausanne, Switzerland

<sup>2</sup> Institute of Pathology, Lausanne University Hospital, Lausanne, Switzerland

<sup>3</sup> Center of Experimental Therapies (CTE), Department of Oncology, Lausanne University Hospital and University of Lausanne, Lausanne, Switzerland

<sup>4</sup> Translational Tumor Immunology Group, Department of Oncology, Lausanne University Hospital, Epalinges, Switzerland

<sup>5</sup> Department of Oncology, Lausanne University Hospital, Lausanne, Switzerland

<sup>6</sup> Department of Thoracic Surgery, Lausanne University Hospital, Lausanne, Switzerland

## Introduction

Non-small-cell lung cancer (NSCLC) accounts for approximately 85% of all lung cancer cases and has the highest incidence amongst malignancies, reaching 13% of all new cancer diagnoses. It is considered the leading cause of cancer-related death worldwide, having a poor prognosis and a 5-year survival rate of 15% in spite of therapeutic advances [1, 2]. Almost 80% of patients with newly diagnosed NSCLC present with disease that is either locally advanced (stage IIIB, 22%) or metastatic (stage IV, 56%), and therefore not amenable to surgical resection [3]. Treatment options available for patients with inoperable disease who are candidates for systemic therapy include platinum-based cytotoxic chemotherapy regimens, molecular targeted agents for patients who carry specific driver mutations and, more recently, immune checkpoint inhibitors [4]. Specifically, immunotherapy with antibodies that prevent the interaction of the programmed death ligand-1 (PD-L1) with the programmed cell death-1 (PD-1) receptor, thus releasing T cells to eliminate tumour cells, has led to significantly improved survival in patients with NSCLC [5–10].

PD-L1 appears to be the main PD-1 ligand expressed in solid tumours, including NSCLC. PD-L1 upregulation in cancer may also be a result of constitutive expression by tumour cells because of genetic alterations or activation of signalling pathways, independently of inflammatory signals in the tumour microenvironment (innate immune resistance) or hypoxia [11], or may be an induced response to inflammatory signals produced by an active antitumour immune response (adaptive immune response) [12, 13].

The overall rate of response of NSCLC to PD-1/PD-L1 blockade is approximately 30% in an unselected population. Thus, there is a need for biomarkers predictive of clinical response. The expression of PD-L1 in formalin-fixed tumour tissue has been shown to be increased in responder NSCLC patients, and is a companion test for one of the commercially available anti-PD-1 antibodies (pembrolizumab) for second-line and even first-line therapy [11, 14]. Recently, the tumour mutational burden, expressed as number of somatic mutations per megabase of tumour DNA, has also been shown to be a potentially useful predictor of response, irrespective of PD-L1 status, to combined CTLA-4 and PD-1 blockade in first-line therapy of metastatic NSCLC [15].

$^{18}\text{F}$ -Fluorodeoxyglucose positron emission tomography/computed tomography ( $^{18}\text{F}$ -FDG PET/CT) is considered the standard modality for staging and follow-up monitoring of NSCLC patients, and has shown high prognostic value based on the different functional parameters analysed, including standardized uptake value (SUV), maximum SUV (SUV<sub>max</sub>), metabolic tumour volume (MTV) and total lesion glycolysis (TLG) [16, 17]. However, the relationship between these metabolic factors and tumour PD-L1 expression in NSCLC so far remains unexplored. Ligation of tumour PD-L1 leads to mTOR activation

and promotion of tumour glycolytic activity [18]. Whether such PD-L1-mediated increase in tumour cell glycolysis is detectable in patients by  $^{18}\text{F}$ -FDG PET/CT is an open question. Studies have shown that PD-L1 may be upregulated in hypoxic tumour tissue via the hypoxia-inducible factor-1 $\alpha$ , making it not only more glycolytic but also more resistant to the adaptive immune system [19]. During aggressive tumour development, hypoxic regions increase as a consequence of progressive restriction of oxygen supply, leading to necrotic cell death in the central tumour compartment [20].

These observations together with the fact that  $^{18}\text{F}$ -FDG PET/CT has the ability to distinguish between viable and nonviable compartments in tumour lesions [21] led us to hypothesize that  $^{18}\text{F}$ -FDG PET/CT could be applied to determine the relative extent of peripheral FDG-avid and central non-FDG-avid compartments as a surrogate marker of the extent of necrosis in tumour lesions. In turn, such a tumour necrosis index might be an indicator of tumour PD-L1 expression. The aim of this study was to investigate the possible association between tumour PD-L1 expression in biopsied or resected tumour lesions from NSCLC patients and  $^{18}\text{F}$ -FDG PET/CT imaging parameters. The relative extent of necrotic and nonnecrotic tumour compartments in the biopsied lesions was also determined.

## Materials and methods

### Patient selection and evaluation of clinical data

We retrospectively analysed 49 patients (28 men, 21 women; median age 68 years, range 40–88 years) diagnosed with NSCLC and treated in a single centre (Thoracic Oncology Clinic at Lausanne University Hospital) between January 2016 and March 2017. Only patients with an initial diagnosis, and not those diagnosed with recurrence, were included in the analysis. Clinical data including type of treatment were obtained in all patients. Radiological outcome in patients undergoing treatment directed at PD1/PD-L1 was evaluated by a board-certified radiologist and a board-certified nuclear medicine physician using iRECIST [22]. Patients were grouped as either experiencing progression of disease (iPD), stable disease (iSD) or partial response/complete response (iPR/iCR). The local Ethics Research Committee of the State of Vaud approved the research protocol (CER-VD #2017-00758). Informed consent was waived due to the retrospective nature of this study.

### $^{18}\text{F}$ -FDG PET/CT

$^{18}\text{F}$ -FDG PET/CT was performed in all patients as part of a standard diagnostic work-up, and patients were categorized based on the American Joint Committee on Cancer (AJCC) TNM staging system. PET/CT was performed using a Discovery D690 TOF (GE HealthCare, Waukesha, WI,

USA) 50–70 min after intravenous injection of a planned  $3.7 \pm 0.5$  MBq/kg of  $^{18}\text{F}$ -FDG. Patients were required to fast for  $\geq 6$  h before the scan. Blood glucose levels were verified with a dedicated electronic glucometer to ensure levels of  $< 8.5$  mmol/L. A low-dose helical CT scan (120–140 kV, 80–200 mA) was first performed for anatomical correlation and attenuation correction. Whole-body emission images were then acquired using seven to nine overlapping bed positions of 2 min each (starting from the top of the skull and ending at the mid-thigh). Images were reconstructed using conventional oncological iterative protocols with body weight-normalized SUV computation.

The following  $^{18}\text{F}$ -FDG PET/CT parameters for the biopsied or resected lesions were measured in each patient: SUV<sub>max</sub> of the lesion, SUV<sub>mean</sub> of the lesion, MTV and TLG with a threshold of 42% of the maximum SUV signal intensity. Morphological tumour volume (MoTV) was calculated based on lesion delineation on CT images [21, 23]. The ratio of metabolically active volume to global lesion volume (termed the metabolic-to-morphological volume ratio, MMVR) was calculated by dividing MTV by MoTV and expressed as a percentage (Fig. 1).

### Tissue PD-L1 expression and necrosis

In our institution, tissue from all patients is stained for PD-L1 as a standard procedure. Available tumour tissue, obtained by either biopsy or surgical resection (30 biopsies and 19 resections in 49 patients), was investigated by immunohistochemistry (IHC) for PD-L1 on formalin-fixed paraffin-embedded (FFPE) samples. PD-L1 expression in tumour cells was assessed using anti-PD-L1 rabbit monoclonal antibody (clone SP263, ready to use; Ventana Medical Systems, Tucson, AZ, USA) on 4- $\mu\text{m}$  sections obtained from FFPE tissue blocks. Immunohistochemical staining was performed using a BenchMark automatic immunostainer (Ventana Medical Systems). Tumour cells expressing PD-L1 were scored by a board-certified pathologist, and the score was expressed as the percentage of total tumour cells. The absence or presence and the percentage of necrosis were recorded by a board-certified pathologist ( $n = 13$ ).

### Multispectral immunofluorescent tissue staining and image analysis

Available FFPE lung tumour tissue (4- $\mu\text{m}$  sections) was subjected to multiplexed staining using an automatic immunostainer (DISCOVERY ULTRA; Ventana Roche, Tucson, AZ, USA). First, heat-induced antigen retrieval in EDTA buffer (pH 8.0) was performed for 92 min at 95 °C. Multiplex staining was performed in consecutive rounds, each round consisting of antigen retrieval, protein blocking, primary antibody incubation, incubation with secondary antibody labelled with horseradish peroxidase (HRP), addition of OPAL reagents and then antibody

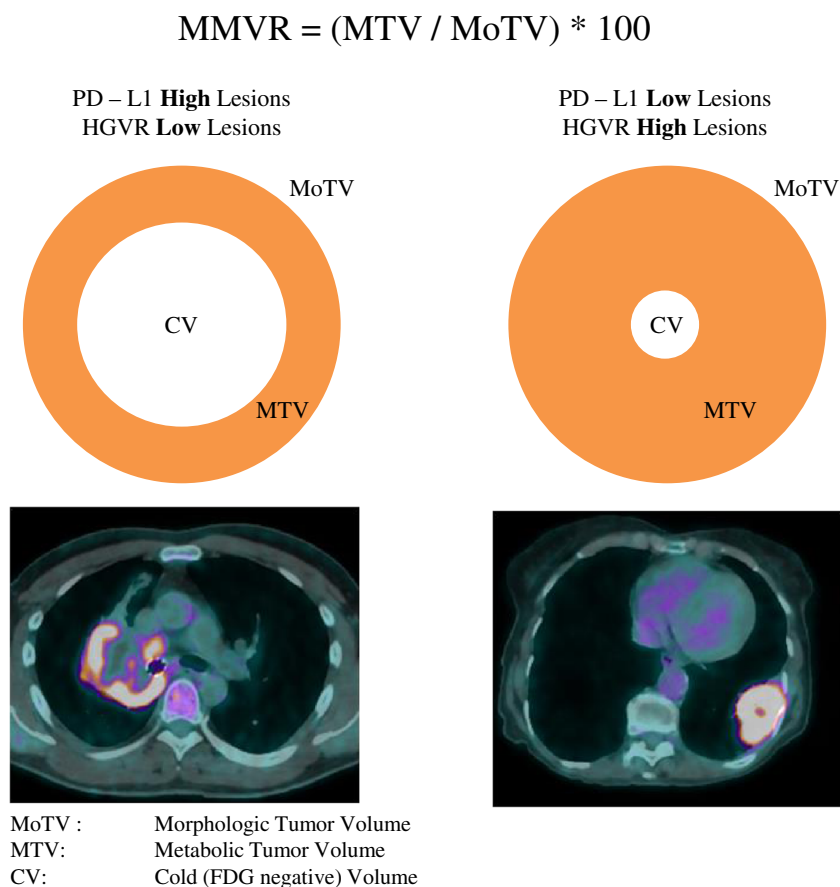
heat denaturation. The monoclonal mouse anti-human PD-1 antibody (0.4  $\mu\text{g}/\text{ml}$ , NAT105; Cell Marque, Rocklin, CA, USA) and mouse monoclonal anti-human granzyme B antibody (1  $\mu\text{g}/\text{ml}$ , Monosan, GrB-7; Uden, The Netherlands) were incubated at room temperature for 60 min, while the rabbit polyclonal anti-human NFATC2 antibody (1  $\mu\text{g}/\text{ml}$ ; Sigma-Aldrich, Saint-Louis, MO, USA), mouse monoclonal anti-pancytokeratin antibody (2  $\mu\text{g}/\text{ml}$ , clone AE1/AE3; Dako, Santa Clara, CA, USA) and rabbit monoclonal anti-CD8 antibody (4  $\mu\text{g}/\text{ml}$ , clone SP16; ThermoFisher Scientific, Waltham, MA, USA) were incubated at 37 °C for 60 min. The signal was revealed by incubation for 16 min with DISCOVERY OmniMap anti-rabbit HRP (Ventana, 760-4311) or anti-mouse HRP (Ventana, 760-4310). Next, the OPAL quality control reagents OPAL 690 (FP1497001KT), OPAL 520 (FP1487001KT), OPAL 540 (FP1494001KT), OPAL 650 (FP1496001KT), OPAL 570 (; all PerkinElmer, Waltham, MA, USA) were added following the manufacturer's recommendations.

Nuclei were visualized by a final incubation with Spectral DAPI (1/10, FP1490, PerkinElmer) for 20 min. Multiplex immunofluorescent (IF) images were acquired on a Vectra 3.0 automatic quantitative pathology imaging system (PerkinElmer). Tissue-specific and panel-specific spectral libraries of individual fluorophores and tumour tissue autofluorescence were acquired for an optimal IF signal unmixing (individual spectral peaks) and multiplex analysis. IF-stained slides were prescanned at  $\times 10$  magnification. Using a Phenochart whole-slide viewer (PerkinElmer), regions of interest containing tumour islets and stroma were marked for high-resolution multispectral acquisition of images at  $\times 20$  magnification. IF signals were extracted using inForm 2.3.0 image analysis software (PerkinElmer) enabling a per-cell analysis of IF markers of multiplex-stained tissue sections. The images were first segmented into tumour and stroma regions, based on cytokeratin staining using the inForm Tissue Finder algorithms. Individual cells were then segmented using the counterstained-based cell segmentation algorithm, based on DAPI staining. Immune cells were quantified using the inForm active learning phenotyping algorithm by assigning the different cell phenotypes across several images or using the scoring tool by defining the threshold of positive IF signal intensity. IF-stained slides were then batch processed, and data were exported and processed via an in-house developed R-script algorithm to retrieve every cell population.

### Statistical analysis

Continuous variables are reported as medians (interquartile range) and dichotomous data as percentages. Metabolic and morphological variables were tested by linear regression analysis as predictors of the percentage of tumour PD-L1 expression in corresponding tissue. The correlations between PD-L1 expression and different metabolic and morphological variables were evaluated using Spearman's rank-order correlation.

**Fig. 1** Intratumoral FDG-avid and FDG non-avid distribution expressed in terms of the metabolic-to-morphological volume ratio (MMVR) in lesions expressing high levels of PD-L1 (PD-L1 high) and low levels of PD-L1 (PD-L1 low). *MTV* metabolic tumour volume, *MoTV* morphological tumour volume, *CV* cold volume (FDG-negative)



The influence of tumour histological subtype on PD-L1 expression and correlation with measured biomarkers were determined for each histological subgroup. Radiological outcomes in patients receiving targeted anti-PD-1/PD-L1 therapy were correlated with the above-mentioned metabolic parameters using Spearman's rank-order correlation. The presence or absence of necrosis was correlated with PD-L1 expression, MoTV, FDG volume, SUVmax, SUVmean and MMVR using the nonparametric Kruskal-Wallis test. The presence of necrosis described in the pathology report was correlated with all investigated imaging factors and PD-L1 expression using Spearman's correlation. All statistical analyses were performed using SPSS software (version 23 for Windows 2010; IBM Corp., Armonk, NY, USA) and STATA version 13.2 (STATA Corp., College Station, TX, USA). Values of  $p < 0.05$  were considered statistically significant.

## Results

### MMVR is inversely correlated with tumour necrosis and PD-L1 expression at baseline

In total, 25 adenocarcinomas (ADC) and 24 squamous cell carcinomas (SCC) were analysed. All tumours showed metabolic

$^{18}\text{F}$ -FDG PET uptake with a mean SUVmax of 13.3 (range 3.3–28.1), SUVmean 7.4 (range 1.9–16.3), MTV 50.3 cm<sup>3</sup> (range 1.2–456 cm<sup>3</sup>) and TLG 283.5 g cm<sup>3</sup>/ml (range 5–2,235 g cm<sup>3</sup>/ml). SUVmax was significantly higher in patients with SCC than in those with ADC ( $p = 0.05$ ). All other imaging parameters, including MMVR ( $p = 0.66$ ), were independent of histological status.

The mean percentage tumour PD-L1 expression in our population of 49 patients was 21.1% (median 3%, range 0–100%) with 19 patients (39%) exceeding 10% expression. The percentage tumour PD-L1 expression was higher in stage IV tumours than in tumours of lower stages (25.3% versus 16.5%, respectively,  $p = 0.03$ ; Table 1). No significant differences in PD-L1 expression were noted among the different histological subgroups ( $p = 0.551$ ).

The two-tailed Spearman's analysis showed a statistically significant negative correlation between the proposed MMVR and PD-L1 tumour expression: tumours with high MMVR expressed significantly lower PD-L1 ( $R = -0.618$ ,  $p < 0.005$ ; Fig. 2). In contrast, there was no significant correlation between PD-L1 tumour expression and any of the following parameters: MTV ( $R = -0.042$ ,  $p = 0.77$ ), TLG ( $R = 0.139$ ,  $p = 0.34$ ), MoTV ( $R = 0.21$ ,  $p = 0.15$ ), SUVmax ( $R = 0.171$ ,  $p = 0.24$ ) or SUVmean ( $R = 0.119$ ,  $p = 0.42$ ). Figure 3 shows a representative tumour with a high MMVR and low PD-L1 expression, and Fig. 4



shows a tumour with a low MMVR and high PD-L1 expression. MMVR predicted PD-L1 expression independently of tumour histological subgroup (ADC or SCC;  $R = -0.991$ ,  $p = 0.020$  for ADC and  $R = -0.760$  for SCC,  $p < 0.005$ ).

As expected, MMVR was inversely correlated with the extent of tumour necrosis ( $R = -0.570$ ,  $p = 0.042$ , Spearman's correlation). PD-L1 expression showed a trend for an association with tumour necrosis ( $R = 0.521$ ,  $p = 0.068$ ). None of the other factors was correlated with the extent of necrosis. Interestingly, PD-L1 expression was not associated with tumour size ( $p = 0.20$ ) measured by the CT component.

### MMVR is inversely correlated with response to PD-1 blockade

Of the 49 patients, 19 were treated with targeted anti-PD-1/PD-L1 therapy. Radiological follow-up was available in 17 of the 19 patients (14 patients, 6 with ADC and 8 with SCC, received anti-

PD-1 therapy including nivolumab or pembrolizumab; 3 patients, 2 with ADC and 1 with SCC, received anti-PD-L1 therapy including atezolizumab or durvalumab). The remaining 30 patients received chemotherapy (adjuvant or palliative), tyrosine kinase Inhibition or resection only in small tumours according to the guidelines. Using iRECIST, 10 of 17 patients showed iPD, 2 iSD, 5 iPR, and 1 iCR. Patients with disease control, i.e. either iSD or iPR/iCR, had a lower MMVR ( $p = 0.043$ , 95% CI  $-0.797$  to  $-0.042$ ) on initial PET/CT than patients with iPD (Fig. 5). None of the other imaging parameters (MTV, TLG, morphological volume, SUVmax and SUVmean) assessed in this analysis was predictive of radiological outcome ( $p = 0.224$ ,  $p = 0.836$ ,  $p = 0.69$ ,  $p = 0.567$  and  $p = 0.586$ , respectively). As expected, patients with disease control also showed higher PD-L1 tumour expression ( $p = 0.033$ , 95% CI  $-0.807$  to  $-0.070$ ).

### Multispectral immunofluorescence tissue staining and image analyses

To further investigate the microenvironment in tumours with high and low MMVR, we performed multispectral IF tissue staining assessing T-cell parameters, i.e. the presence of intratumoral and stromal CD8 tumour-infiltrating lymphocytes (TILs) and their activation status in situ based on expression of granzyme-B (a feature of activated effector cells [24]), expression of PD1 (a feature of antigen-activated TILs [25]), and/or nuclear localization of the transcription factor NFATC2 (a feature of recent engagement of the T-cell receptor by cognate antigen). Of 14 samples available for analysis, nine showed necrosis detected by clinical pathologists, and five showed no necrosis.

A higher density of stromal CD8<sup>+</sup>PD1<sup>+</sup> ( $p = 0.01$ ), CD8<sup>+</sup>GrzB<sup>+</sup> ( $p = 0.031$ ), CD8<sup>+</sup>GrzB<sup>+</sup>PD1<sup>+</sup> ( $p = 0.0081$ ) and CD8<sup>+</sup>NFAT<sup>+</sup>GrzB<sup>+</sup>PD1<sup>+</sup> ( $p = 0.0109$ ) (Fig. 6a) was apparent in tumours with necrotic areas reported than in tumours with no necrotic areas reported (Supplementary Figs. 1 and 2). Moreover, higher densities of intratumoral CD8<sup>+</sup>PD1<sup>+</sup> ( $p = 0.0023$ ), CD8<sup>+</sup>GrzB<sup>+</sup> ( $p = 0.0016$ ), CD8<sup>+</sup>GrzB<sup>+</sup>PD1<sup>+</sup> ( $p = 0.004$ ) (Fig. 6a) were also found in tumours with necrotic areas reported than in tumours with no necrotic areas reported (Supplementary Figs. 1 and 2). The analysis of tumours with a high MMVR in relation to those with a low MMVR based on median cutoff (11.4%) revealed higher mean values for all CD8<sup>+</sup> subgroups in tumours with a low MMVR, although the difference did not reach significance (all  $p > 0.1$ , Fig. 6b).

### Discussion

Although <sup>18</sup>F-FDG PET/CT is used as a standard imaging modality for staging NSCLC, few data are available addressing its potential utility in the evaluation of immune regulatory molecule expression, in particular PD-L1 [26]. Importantly, we showed in this study that MMVR (but not MTV or TLG)

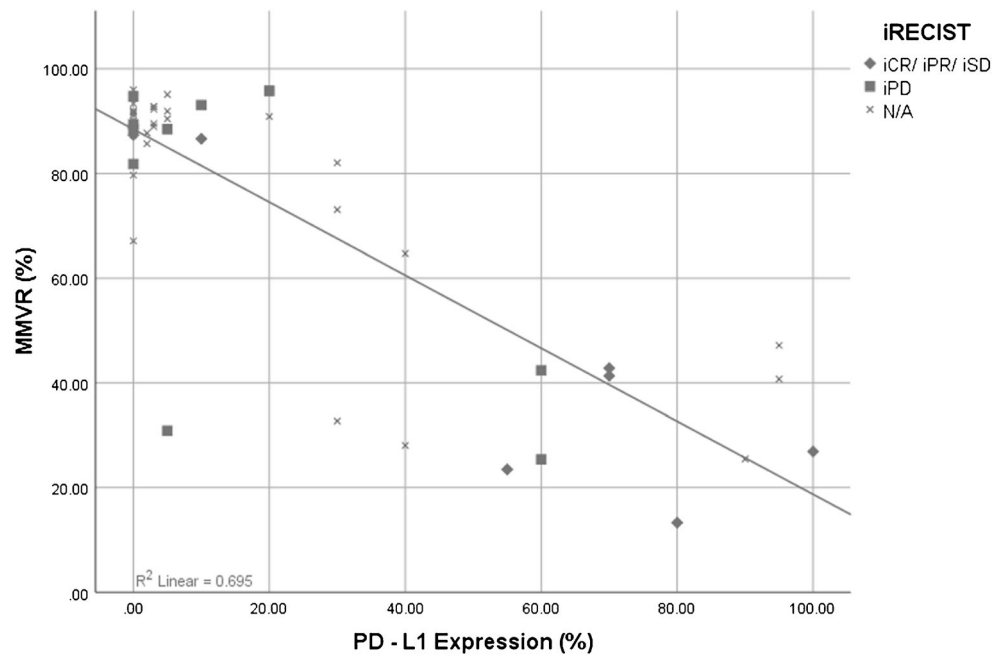
**Table 1** Population characteristics

Characteristic	Value
Demographic parameters	
Number of patients	49
Age (years)	67 (40–88)
Male	28 (57)
Female	21 (43)
Sampling	
Surgical resection	19 (39)
Biopsy	30 (61)
Histological type	
Adenocarcinoma	25 (51)
Squamous cell carcinoma	24 (49)
Stage	
Ia	2 (4)
Ib	2 (4)
IIa	3 (6)
IIb	5 (10)
IIIa	8 (16)
IIIb	3 (6)
IV	26 (53)
Morphological tumour volume (cm <sup>3</sup> )	77.69 (1.4–522)
Metabolic tumour volume (cm <sup>3</sup> )	50.3 (1.2–456)
Tumour SUVmax	13.3 (3.3–28.1)
TLG (g cm <sup>3</sup> /ml)	283.5 (5.04–2230)
MMVR	0.74 (0.13–0.96)
PD-L1 expression (%)	21.4 (0–100)
>10	19 (38)
<10	30 (62)

The values presented are median (interquartile range) or number (%)

TLG total lesion glycolysis, MMVR metabolic-to-morphological volume ratio

**Fig. 2** Relationship between metabolic-to-morphological volume ratio (MMVR) expressed as a percentage and the percentage PD-L1 tumour expression assessed using anti-PD-L1 rabbit monoclonal antibody (clone SP263, ready to use; Ventana Medical Systems, Tucson, AZ, USA) (Spearman's  $\rho = -0.618$ ,  $p < 0.005$ ). Outcomes using iRECIST on follow-up CT in various patients are coded as follows: *diamonds* complete response, *partial response* or *stable disease*, *squares* progressive disease. *N/A* not available



is negatively correlated with tumour PD-L1 expression. To the best of our knowledge, this is the first study to investigate the utility of  $^{18}\text{F}$ -FDG PET/CT metabolic biomarkers in the evaluation and characterization of PD-L1 expression in NSCLC [27]. In this specific patient population, predictive markers of response to anti-PD-1/PD-L1 therapies would be highly

valuable, as they are the cornerstone for the selection of patients likely to respond to these immunotherapies. Indeed, albeit in a small number of patients, our findings indicate that among all  $^{18}\text{F}$ -FDG PET imaging parameters at baseline, only

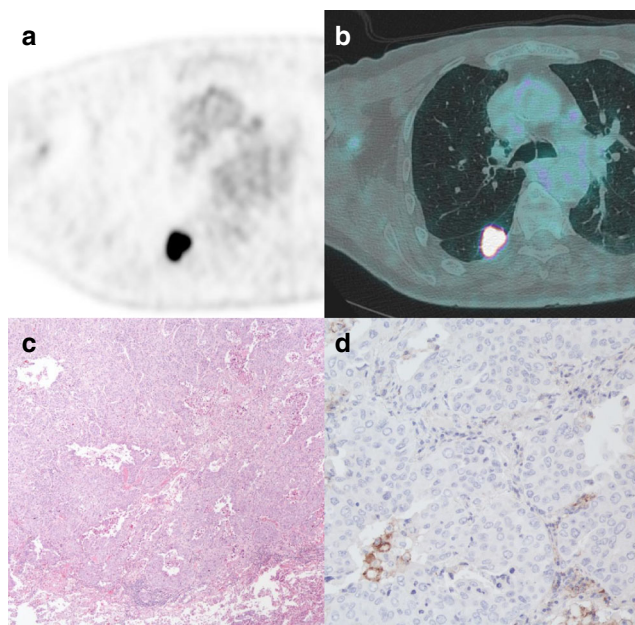


**Fig. 3** Representative tumour with a high MMVR and low PD-L1 expression. **a, b** PET (**a**) and PET/CT (**b**) images show homogeneously high FDG uptake within the pulmonary mass (SUVmax 24.1, tumour morphological volume  $8.7 \text{ cm}^3$ , tumour metabolic volume  $8.2 \text{ cm}^3$ ) and high MMVR (94%). **c, d** Pathological examination of the resected mass shows (**c**) adenocarcinoma with a solid growth pattern (H&E,  $\times 20$ ) demonstrating (**d**) 5% PD-L1 expression (PD-L1 SP263 immunohistochemical staining,  $\times 100$ )

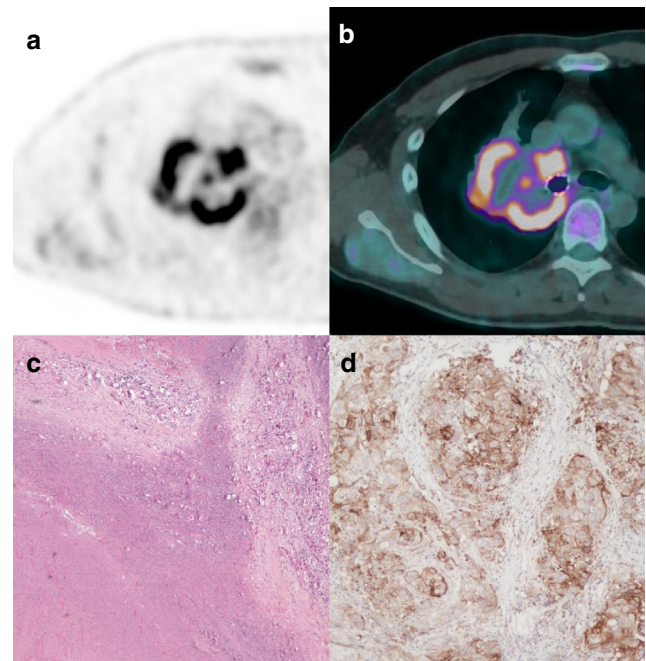
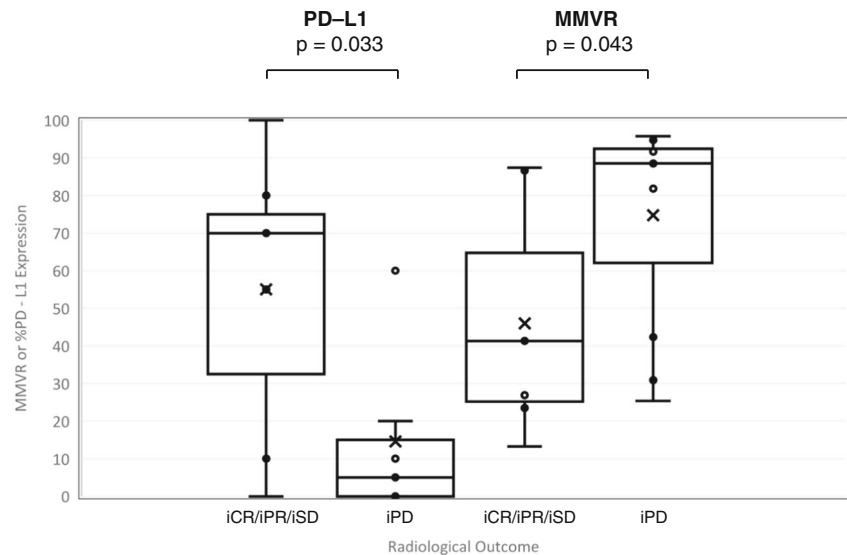


**Fig. 4** Representative tumour with a low MMVR and high PD-L1 expression. **a, b** PET (**a**) and PET/CT (**b**) images show high peripheral FDG uptake within the pulmonary mass, with central regions lacking tracer uptake (SUVmax 17.2, tumour morphological volume  $291 \text{ cm}^3$ , tumour metabolic volume  $38.6 \text{ cm}^3$ ) and low MMVR (13.3%). **c, d** Pathological examination of the resected mass shows (**c**) a poorly differentiated NSCLC at the border of the necrotic core and viable cells (H&E,  $\times 20$ ) demonstrating (**d**) 80% PD-L1 expression ( $\times 100$ )

**Fig. 5** Mean PD-L1 expression and MMVR in tumours showing benefit by immune-related response criteria (*iCR* complete response, *iPR* partial response, *iSD* stable disease) and tumours showing progression of disease (*iPD*).  $p = 0.033$  and  $p = 0.043$ , respectively



MMVR was able to predict radiological response to PD-L1/PD-1 blockade, as assessed by the iRECIST criteria. This suggests that a low MMVR at baseline is a promising parameter for the identification of patients who have a higher chance of responding to immunotherapy with anti-PD-L1/PD-1 blocking antibodies, and this application should be explored further.

Our findings likely reflect the underlying biology linking steady-state biological activity of tumours with baseline immune recognition and response to checkpoint immunotherapy. Indeed, we found an inverse correlation between MMVR and expression of PD-L1 in tumours, an established biomarker that can predict response to PD-1 blockade in NSCLC patients [28–30]. Furthermore, a correlation between PD-L1 expression and response has been shown in the KEYNOTE-001 trial, and our finding that PD-L1 expression (and consequently MMVR) predict response in a mixed ADC/SCC population is in accordance with the finding of the KEYNOTE-001 study [8]. Importantly, no correlation was found between PD-L1 expression and other imaging parameters including MTV, TLG, SUVmax and SUVmean of tumour tissue. These findings indicate that the presence of important areas of reduced metabolic activity in tumours, which lead to low MMVR, predict immunoreactivity at baseline and consequently response to PD-1 blockade. We hypothesized that such an imaging pattern would reflect tumour necrosis [21], and in fact, low MMVR was found in tumours with documented necrotic areas by H&E, whereas tumours lacking features of necrosis exhibited high MMVR.

Tumour necrosis has been described as a predictor of aggressive tumour behaviour and reduced survival in patients with NSCLC, even though the independent prognostic significance of this biomarker in NSCLC has not yet been firmly established [31]. The prognostic significance of necrosis has been demonstrated statistically in several studies [32–36]. Necrosis has also been correlated with tumour recurrence

and with metastatic disease [26, 37, 38]. Moreover, other studies have shown that a high apoptotic index (AI) in NSCLC is an independent prognostic factor for shortened survival with worse local control and a higher number of distant metastases [32, 39]. Furthermore, it has been reported that NSCLC patients with very high AI values combined with a very high proliferating cell nuclear antigen (PCNA) labelling index have a particularly poor overall prognosis [40].

Necrosis can trigger inflammation, facilitating influx of T cells and upregulation of PD-L1 [41] over local tumour necrosis factor  $\alpha$  (TNF- $\alpha$ ). TNF- $\alpha$  is a major inflammatory cytokine that was first identified because of its ability to induce rapid haemorrhagic necrosis, which might be a relevant factor. Indeed, PD-L1 is upregulated in hypoxic tissue [19]. In our patient population there was a trend for PD-L1 expression to be correlated with the presence of necrosis. This is in agreement with the finding of a recent study in 122 patients with pulmonary pleomorphic carcinoma showing a significant correlation between high PD-L1 expression and tumour necrosis [42]. Another study has also shown that inflammatory cytokines IL-17 and TNF- $\alpha$  directly upregulate PD-L1 expression in human prostate and colon cancer cell lines [43].

To further explore whether necrosis and increased PD-L1 expression was associated with increased infiltration and activation of CD8<sup>+</sup> T cells in NSCLC, we analysed the tumour T-cell contexture using multiplex cellular staining. We found a significantly higher influx of activated CD8<sup>+</sup> T cells in the stromal compartment as well as in the tumour compartment of tumours that exhibited areas of necrosis than in tumours that exhibited no necrosis on histological examination. This finding may be related to necrosis triggering the release of tumour antigens and boosting the tumour immunity cycle [44]. In turn, effective T-cell activation may feed forward the immunity cycle thus amplifying the necrotic process and, by virtue of the localized released of IFN- $\gamma$ , induce additional

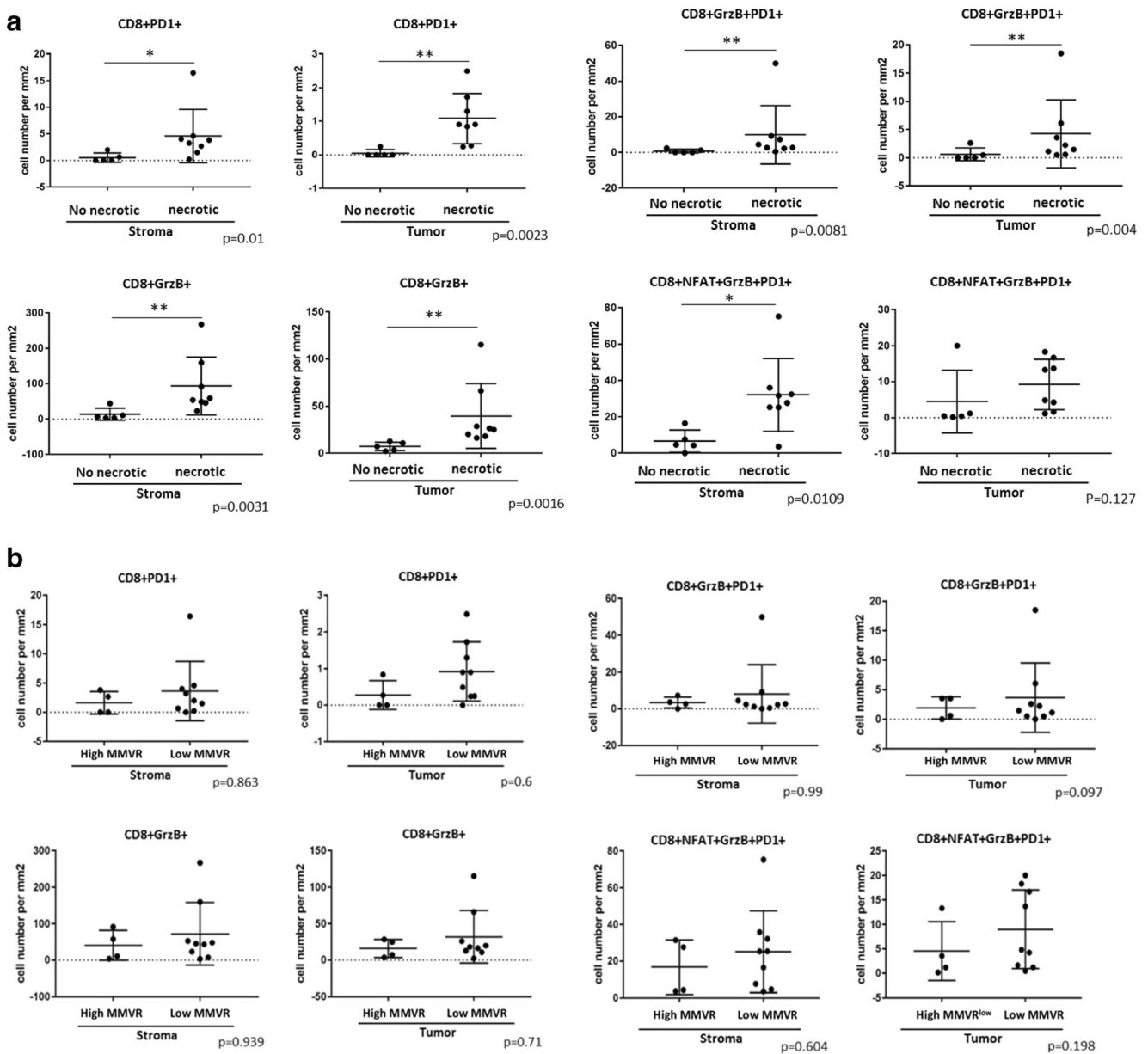


**Fig. 6** Multispectral Immunofluorescence tissue staining of (a) tumour samples with and without necrosis ( $*p < 0.05$ ,  $**p < 0.01$ ) and (b) tumour samples with a high MMVR ( $n = 4$ ) and a low MMVR ( $n = 9$ ; all  $p > 0.1$ )

PD-L1 on viable tumour cells. While low MMVR did not significantly predict influx of activated CD8<sup>+</sup> T cells, there was a trend for tumours with low MMVR to exhibit higher CD8<sup>+</sup> TIL subpopulations. We suspect that the low number of samples available for this study led to the analysis being underpowered. We aim to overcome this shortcoming resulting from the retrospective nature of this exploratory analysis by establishing a large prospective database analysing these imaging markers in a broader population. This might also elucidate how possible bias towards earlier disease because of the analysis of resectable cases might have played a role in the present analysis.

MMVR, introduced here, is an expression of the percentage of tumour volume that is metabolically active, most likely indirectly reflecting the extent of complementary regions that are metabolically inactive and presumably prone to necrosis and apoptotic events in the global tumour volume. The current analysis thus identified a new biomarker, MMVR, as a predictor of tumour PD-L1 expression and clinical outcome following PD-1/PD-L1 blockade in lung cancer. In clinical practice, it could be used to guide biopsy testing for PD-L1 expression, and to identify patients who could potentially benefit from therapy directed at PD-L1/PD-1.



## Conclusion

This study identified a new non-invasive imaging-based biomarker which correlates with the expression of PD-L1 and response to PD-1/PD-L1 blockade in patients with advanced stage NSCLC. The negative correlation between tumour PD-L1 expression and the FDG-avid tumour volume expressed by MMVR could reveal intratumoral necrotic and/or apoptotic changes and their possible association with tumour inflammation, T-cell infiltration and PD-L1 expression. Further investigation is needed to confirm these possible associations and to elucidate in a larger number of patients the role of MMVR as a predictor of PD-L1 expression and clinical response to targeted anti-PD-1/PD-L1 therapy.

## Compliance with ethical standards

**Conflicts of interest** None.

**Ethical approval** All procedures performed in studies involving human participants were in accordance with the ethical standards of the institutional and/or national research committee and with the principles of the 1964 Declaration of Helsinki and its later amendments or comparable ethical standards.

**Informed consent** Informed consent was waived due to the retrospective nature of this study.

## References

- Siegel RL, Miller KD, Jemal A. Cancer statistics, 2016. *CA Cancer J Clin*. 2016;66:7–30. <https://doi.org/10.3322/caac.21332>.
- Didkowska J, Wojciechowska U, Manczuk M, Lobaszewski J. Lung cancer epidemiology: contemporary and future challenges worldwide. *Ann Transl Med*. 2016;4:150. <https://doi.org/10.21037/atm.2016.03.11>.
- Scagliotti GV, Bironzo P, Vansteenkiste JF. Addressing the unmet need in lung cancer: the potential of immuno-oncology. *Cancer Treat Rev*. 2015;41:465–75. <https://doi.org/10.1016/j.ctrv.2015.04.001>.
- Brahmer JR, Pardoll DM. Immune checkpoint inhibitors: making immunotherapy a reality for the treatment of lung cancer. *Cancer Immunol Res*. 2013;1:85–91. <https://doi.org/10.1158/2326-6066.cir-13-0078>.
- Topalian SL, Hodi FS, Brahmer JR, Gettinger SN, Smith DC, McDermott DF, et al. Safety, activity, and immune correlates of anti-PD-1 antibody in cancer. *N Engl J Med*. 2012;366:2443–54. <https://doi.org/10.1056/NEJMoa1200690>.
- Brahmer J, Reckamp KL, Baas P, Crino L, Eberhardt WE, Poddubskaya E, et al. Nivolumab versus docetaxel in advanced squamous-cell non-small-cell lung cancer. *N Engl J Med*. 2015;373:123–35. <https://doi.org/10.1056/NEJMoa1504627>.
- Borghaei H, Paz-Ares L, Horn L, Spigel DR, Steins M, Ready NE, et al. Nivolumab versus docetaxel in advanced nonsquamous non-small-cell lung cancer. *N Engl J Med*. 2015;373:1627–39. <https://doi.org/10.1056/NEJMoa1507643>.
- Garon EB, Rizvi NA, Hui R, Leighl N, Balmanoukian AS, Eder JP, et al. Pembrolizumab for the treatment of non-small-cell lung cancer. *N Engl J Med*. 2015;372:2018–28. <https://doi.org/10.1056/NEJMoa1501824>.
- Brahmer JR, Tykodi SS, Chow LQ, Hwu WJ, Topalian SL, Hwu P, et al. Safety and activity of anti-PD-L1 antibody in patients with advanced cancer. *N Engl J Med*. 2012;366:2455–65. <https://doi.org/10.1056/NEJMoa1200694>.
- Soria JC, Marabelle A, Brahmer JR, Gettinger S. Immune checkpoint modulation for non-small cell lung cancer. *Clin Cancer Res*. 2015;21:2256–62. <https://doi.org/10.1158/1078-0432.ccr-14-2959>.
- Barsoum IB, Smallwood CA, Siemens DR, Graham CH. A mechanism of hypoxia-mediated escape from adaptive immunity in cancer cells. *Cancer Res*. 2014;74:665–74. <https://doi.org/10.1158/0008-5472.can-13-0992>.
- Anagnostou VK, Brahmer JR. Cancer immunotherapy: a future paradigm shift in the treatment of non-small cell lung cancer. *Clin Cancer Res*. 2015;21:976–84. <https://doi.org/10.1158/1078-0432.ccr-14-1187>.
- Remon J, Chaput N, Planchard D. Predictive biomarkers for programmed death-1/programmed death ligand immune checkpoint inhibitors in nonsmall cell lung cancer. *Curr Opin Oncol*. 2016;28:122–9. <https://doi.org/10.1097/cco.0000000000000263>.
- Herbst RS, Baas P, Kim DW, Felip E, Pérez-Gracia JL, Han JY, et al. Pembrolizumab versus docetaxel for previously treated, PD-L1-positive, advanced non-small-cell lung cancer (KEYNOTE-010): a randomised controlled trial. *Lancet*. 2016;387(10027):1540–50. [https://doi.org/10.1016/S0140-6736\(15\)01281-7](https://doi.org/10.1016/S0140-6736(15)01281-7).
- Pai-Scherf L, Blumenthal GM, Li H, Subramaniam S, Mishra-Kalyani PS, He K, et al. FDA approval summary: Pembrolizumab for treatment of metastatic non-small cell lung cancer: first-line therapy and beyond. *Oncologist*. 2017;22(11):1392–9. <https://doi.org/10.1634/theoncologist.2017-0078>.
- Hellmann MD, Ciuleanu TE, Pluzanski A, Lee JS, Otterson GA, Audigier-Valette C, et al. Nivolumab plus Ipilimumab in lung cancer with a high tumor mutational burden. *N Engl J Med*. 2018;378(22):2093–104. <https://doi.org/10.1056/NEJMoa1801946>.
- Davison J, Mercier G, Russo G, Subramaniam RM. PET-based primary tumor volumetric parameters and survival of patients with non-small cell lung carcinoma. *AJR Am J Roentgenol*. 2013;200:635–40. <https://doi.org/10.2214/ajr.12.9138>.
- Zhu A, Lee D, Shim H. Metabolic positron emission tomography imaging in cancer detection and therapy response. *Semin Oncol*. 2011;38:55–69. <https://doi.org/10.1053/j.seminoncol.2010.11.012>.
- Chang CH, Qiu J, O’Sullivan D, Buck MD, Noguchi T, Curtis JD, et al. Metabolic competition in the tumor microenvironment is a driver of cancer progression. *Cell*. 2015;162(6):1229–41. <https://doi.org/10.1016/j.cell.2015.08.016>.
- Steinbach JP, Wolburg H, Klumpp A, Probst H, Weller M. Hypoxia-induced cell death in human malignant glioma cells: energy deprivation promotes decoupling of mitochondrial cytochrome c release from caspase processing and necrotic cell death. *Cell Death Differ*. 2003;10:823–32. <https://doi.org/10.1038/sj.cdd.4401252>.
- Soussan M, Cyrta J, Pouliquen C, Chouahnia K, Orhac F, Martinod E, et al. Fluorine 18 fluorodeoxyglucose PET/CT volume-based indices in locally advanced non-small cell lung cancer: prediction of residual viable tumor after induction chemotherapy. *Radiology*. 2014;272:875–84. <https://doi.org/10.1148/radiol.1413219>.
- Seymour L, Bogaerts J, Perrone A, Ford R, Schwartz LH, Mandrekar S, et al. iRECIST: guidelines for response criteria for use in trials testing immunotherapeutics. *Lancet Oncol*. 2017;18(3):e143–52. [https://doi.org/10.1016/S1470-2045\(17\)30074-8](https://doi.org/10.1016/S1470-2045(17)30074-8).
- Xie X, Willemink MJ, de Jong PA, van Ooijen PM, Oudkerk M, Vliegenthart R, et al. Small irregular pulmonary nodules in low-dose CT: observer detection sensitivity and volumetry accuracy. *AJR Am J Roentgenol*. 2014;202:W202–9. <https://doi.org/10.2214/ajr.13.10830>.
- Mami-Chouaib F, Blanc C, Corgnac S, et al. Resident memory T cells, critical components in tumor immunology. *J Immunother Cancer*. 2018;6:87–97. <https://doi.org/10.1186/s40425-018-0399-6>.

25. Speiser DE, Ho PC, Verdeil G. Regulatory circuits of T cell function in cancer. *Nat Rev Immunol*. 2016;16(10):599–611. <https://doi.org/10.1038/nri.2016.80>.
26. Sheikhabaehi S, Mena E, Yanamadala A, Reddy S, Solnes LB, Wachsmann J, et al. The value of FDG PET/CT in treatment response assessment, follow-up, and surveillance of lung cancer. *AJR Am J Roentgenol*. 2017;208:420–33. <https://doi.org/10.2214/ajr.16.16532>.
27. Ilie M, Hofman V, Dietel M, Soria JC, Hofman P. Assessment of the PD-L1 status by immunohistochemistry: challenges and perspectives for therapeutic strategies in lung cancer patients. *Virchows Arch*. 2016;468:511–25. <https://doi.org/10.1007/s00428-016-1910-4>.
28. Passiglia F, Bronte G, Bazan V. PD-L1 expression as predictive biomarker in patients with NSCLC: a pooled analysis. *Oncotarget*. 2016;7(15):19738–47. <https://doi.org/10.18632/oncotarget.7582>.
29. Zhou ZJ, Zhan P, Song Y. PD-L1 over-expression and survival in patients with non-small cell lung cancer: a meta-analysis. *Transl Lung Cancer Res*. 2015;4:203–8. <https://doi.org/10.3978/j.issn.2218-6751.2015.03.02>.
30. Wang A, Wang HY, Liu Y, Zhao MC, Zhang HJ, Lu ZY, et al. The prognostic value of PD-L1 expression for non-small cell lung cancer patients: a meta-analysis. *Eur J Surg Oncol*. 2015;41:450–6. <https://doi.org/10.1016/j.ejso.2015.01.020>.
31. Gkogkou C, Frangia K, Saif MW, Trigidou R, Syrigos K. Necrosis and apoptotic index as prognostic factors in non-small cell lung carcinoma: a review. *Springerplus*. 2014;3:120. <https://doi.org/10.1186/2193-1801-3-120>.
32. Tormanen U, Eerola AK, Rainio P, Vahakangas K, Soini Y, Sormunen R, et al. Enhanced apoptosis predicts shortened survival in non-small cell lung carcinoma. *Cancer Res*. 1995;55:5595–602.
33. Cho S, Sung SW, Jheon S, Chung JH. Risk of recurrence in surgically resected stage I adenocarcinoma of the lung: histopathologic and immunohistochemical analysis. *Lung*. 2008;186:411–9. <https://doi.org/10.1007/s00408-008-9116-4>.
34. Kilicgun A, Turma A, Sayar A, Solak O, Urer N, Gurses A. Very important histopathological factors in patients with resected non-small cell lung cancer: necrosis and perineural invasion. *Thorac Cardiovasc Surg*. 2010;58:93–7. <https://doi.org/10.1055/s-0029-1186240>.
35. Park SY, Lee HS, Jang HJ, Lee GK, Chung KY, Zo JI. Tumor necrosis as a prognostic factor for stage IA non-small cell lung cancer. *Ann Thorac Surg*. 2011;91:1668–73. <https://doi.org/10.1016/j.athoracsur.2010.12.028>.
36. Pataer A, Kalhor N, Correa AM, Raso MG, Erasmus JJ, Kim ES, et al. Histopathologic response criteria predict survival of patients with resected lung cancer after neoadjuvant chemotherapy. *J Thorac Oncol*. 2012;7:825–32. <https://doi.org/10.1097/JTO.0b013e318247504a>.
37. Tantraworasin A, Saeteng S, Lertprasertsuke N, Arreyakajohn N, Kasemsam C, Patumanond J. Prognostic factors of tumor recurrence in completely resected non-small cell lung cancer. *Cancer Manag Res*. 2013;5:77–84. <https://doi.org/10.2147/cmar.s45642>.
38. Swinson DE, Jones JL, Richardson D, Cox G, Edwards JG, O'Byrne KJ. Tumour necrosis is an independent prognostic marker in non-small cell lung cancer: correlation with biological variables. *Lung Cancer*. 2002;37:235–40.
39. Langendijk H, Thunnissen E, Arends JW, de Jong J, ten Velde G, Lamers R, et al. Cell proliferation and apoptosis in stage III inoperable non-small cell lung carcinoma treated by radiotherapy. *Radiother Oncol*. 2000;56:197–207.
40. Dworakowska D, Jassem E, Jassem J, Karmolinski A, Lapinski M, Tomaszewski D, et al. Prognostic value of the apoptotic index analysed jointly with selected cell cycle regulators and proliferation markers in non-small cell lung cancer. *Lung Cancer*. 2009;66:127–33. <https://doi.org/10.1016/j.lungcan.2009.01.008>.
41. Garg AD, Agostinis P. Cell death and immunity in cancer: from danger signals to mimicry of pathogen defense responses. *Immunol Rev*. 2017;280(1):126–48. <https://doi.org/10.1111/imr.12574>.
42. Chang YL, Yang CY, Lin MW, Wu CT, Yang PC. High co-expression of PD-L1 and HIF-1 $\alpha$  correlates with tumour necrosis in pulmonary pleomorphic carcinoma. *Eur J Cancer*. 2016;60:125–35. <https://doi.org/10.1016/j.ejca.2016.03.012>.
43. Wang V, Yang L, Huang F, Zhang Q, Liu S, Ma L, et al. Inflammatory cytokines IL-17 and TNF- $\alpha$  up-regulate PD-L1 expression in human prostate and colon cancer cells. *Immunol Lett*. 2017;184:7–14. <https://doi.org/10.1016/j.imlet.2017.02.006>.
44. Chen DS, Mellman I. Oncology meets immunology: the cancer-immunity cycle. *Immunity*. 2013;39(1):1–10. <https://doi.org/10.1016/j.immuni.2013.07.012>.

**Publisher's note** Springer Nature remains neutral with regard to jurisdictional claims in published maps and institutional affiliations.